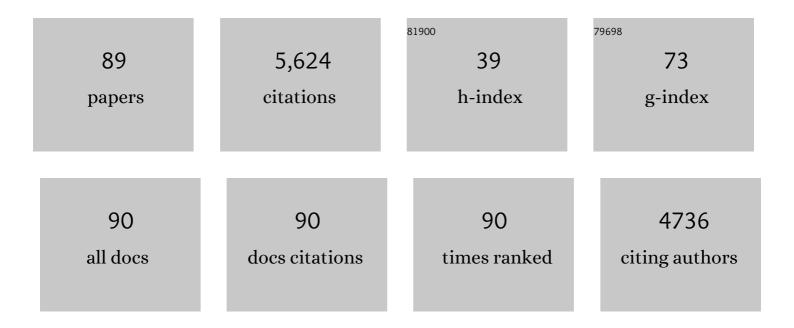
Andrew J Burghardt

List of Publications by Year in descending order

Source: https://exaly.com/author-pdf/5431508/publications.pdf Version: 2024-02-01



#	Article	IF	CITATIONS
1	CT Muscle Density, D3Cr Muscle Mass, and Body Fat Associations With Physical Performance, Mobility Outcomes, and Mortality Risk in Older Men. Journals of Gerontology - Series A Biological Sciences and Medical Sciences, 2022, 77, 790-799.	3.6	13
2	Biochemical Markers of Bone Turnover in Older Adults With Type 1 Diabetes. Journal of Clinical Endocrinology and Metabolism, 2022, 107, e2405-e2416.	3.6	9
3	Interpretation of Bone Mineral Density Z-Scores by Dual-Energy X-Ray Absorptiometry in Transgender and Gender Diverse Youth Prior to Gender-Affirming Medical Therapy. Journal of Clinical Densitometry, 2022, 25, 559-568.	1.2	4
4	Reliability and Change in Erosion Measurements by High-resolution Peripheral Quantitative Computed Tomography in a Longitudinal Dataset of Rheumatoid Arthritis Patients. Journal of Rheumatology, 2021, 48, 348-351.	2.0	6
5	Longitudinal Evolution of Bone Microarchitecture and Bone Strength in Type 2 Diabetic Postmenopausal Women With and Without History of Fragility Fractures—A 5-Year Follow-Up Study Using High Resolution Peripheral Quantitative Computed Tomography. Frontiers in Endocrinology, 2021, 12, 599316.	3.5	13
6	Global and Spatial Compartmental Interrelationships of Bone Density, Microstructure, Geometry and Biomechanics in the Distal Radius in a Colles' Fracture Study Using HR-pQCT. Frontiers in Endocrinology, 2021, 12, 568454.	3.5	1
7	Differences in bone mineral density and morphometry measurements by fixed versus relative offset methods in high-resolution peripheral quantitative computed tomography. Bone, 2021, 149, 115973.	2.9	4
8	Augmenting Osteoporosis Imaging with Machine Learning. Current Osteoporosis Reports, 2021, 19, 699-709.	3.6	1
9	HRâ€pQCT Measures of Bone Microarchitecture Predict Fracture: Systematic Review and Metaâ€Analysis. Journal of Bone and Mineral Research, 2020, 35, 446-459.	2.8	92
10	Objective measures of moderate to vigorous physical activity are associated with higher distal limb bone strength among elderly men. Bone, 2020, 132, 115198.	2.9	5
11	High-Resolution Peripheral Quantitative Computed Tomography for Bone Evaluation in Inflammatory Rheumatic Disease. Frontiers in Medicine, 2020, 7, 337.	2.6	32
12	Consensus approach for 3D joint space width of metacarpophalangeal joints of rheumatoid arthritis patients using high-resolution peripheral quantitative computed tomography. Quantitative Imaging in Medicine and Surgery, 2020, 10, 314-325.	2.0	23
13	Hip Fracture Discrimination Based on Statistical Multi-parametric Modeling (SMPM). Annals of Biomedical Engineering, 2019, 47, 2199-2212.	2.5	11
14	Structural Changes over a Short Period Are Associated with Functional Assessments in Rheumatoid Arthritis. Journal of Rheumatology, 2019, 46, 676-684.	2.0	12
15	Volumetric Bone Mineral Density and Failure Load of Distal Limbs Predict Incident Clinical Fracture Independent of FRAX and Clinical Risk Factors Among Older Men. Journal of Bone and Mineral Research, 2018, 33, 1302-1311.	2.8	57
16	High-Resolution Imaging Techniques for Bone Quality Assessment. , 2018, , 1007-1041.		3
17	Accelerated Bone Loss in Older Men: Effects on Bone Microarchitecture and Strength. Journal of Bone and Mineral Research, 2018, 33, 1859-1869.	2.8	12
18	Quantitative characterization of metacarpal and radial bone in rheumatoid arthritis using high resolution- peripheral quantitative computed tomography. International Journal of Rheumatic Diseases, 2017, 20, 353-362.	1.9	16

ANDREW J BURGHARDT

#	Article	IF	CITATIONS
19	The comparability of HR-pQCT bone measurements is improved by scanning anatomically standardized regions. Osteoporosis International, 2017, 28, 2115-2128.	3.1	35
20	Quantifying sex, race, and age specific differences in bone microstructure requires measurement of anatomically equivalent regions. Bone, 2017, 101, 206-213.	2.9	26
21	The SPECTRA Collaboration OMERACT Special Interest Group: Current Research and Future Directions. Journal of Rheumatology, 2017, 44, 1911-1915.	2.0	11
22	Super-resolution/segmentation of 3D trabecular bone images with total variation and nonconvex Cahn-Hilliard functional. , 2017, , .		3
23	Statistical Parametric Mapping of HR-pQCT Images: A Tool for Population-Based Local Comparisons of Micro-Scale Bone Features. Annals of Biomedical Engineering, 2017, 45, 949-962.	2.5	9
24	Operator variability in scan positioning is a major component of HR-pQCT precision error and is reduced by standardized training. Osteoporosis International, 2017, 28, 245-257.	3.1	33
25	Assessment of 3-month changes in bone microstructure under anti-TNFα therapy in patients with rheumatoid arthritis using high-resolution peripheral quantitative computed tomography (HR-pQCT). Arthritis Research and Therapy, 2017, 19, 222.	3.5	27
26	Microarchitecture and Peripheral BMD are Impaired in Postmenopausal White Women With Fracture Independently of Total Hip <i>T</i> -Score: An International Multicenter Study. Journal of Bone and Mineral Research, 2016, 31, 1158-1166.	2.8	69
27	Kartogenin treatment prevented joint degeneration in a rodent model of osteoarthritis: A pilot study. Journal of Orthopaedic Research, 2016, 34, 1780-1789.	2.3	37
28	Bone microstructure in men assessed by HR-pQCT: Associations with risk factors and differences between men with normal, low, and osteoporosis-range areal BMD. Bone Reports, 2016, 5, 312-319.	0.4	7
29	Cortical bone laminar analysis reveals increased midcortical and periosteal porosity in type 2 diabetic postmenopausal women with history of fragility fractures compared to fracture-free diabetics. Osteoporosis International, 2016, 27, 2791-2802.	3.1	47
30	Determining Metacarpophalangeal Flexion Angle Tolerance for Reliable Volumetric Joint Space Measurements by High-resolution Peripheral Quantitative Computed Tomography. Journal of Rheumatology, 2016, 43, 1941-1944.	2.0	10
31	Serum miRNA Signatures Are Indicative of Skeletal Fractures in Postmenopausal Women With and Without Type 2 Diabetes and Influence Osteogenic and Adipogenic Differentiation of Adipose Tissue–Derived Mesenchymal Stem Cells In Vitro. Journal of Bone and Mineral Research, 2016, 31, 2173-2192.	2.8	115
32	Correlation of structural abnormalities of the wrist and metacarpophalangeal joints evaluated by high-resolution peripheral quantitative computed tomography, 3ÂTesla magnetic resonance imaging and conventional radiographs in rheumatoid arthritis. International Journal of Rheumatic Diseases, 2015, 18, 628-639.	1.9	33
33	Validation of bone marrow fat quantification in the presence of trabecular bone using MRI. Journal of Magnetic Resonance Imaging, 2015, 42, 539-544.	3.4	65
34	Semi-blind joint super-resolution/segmentation of 3D trabecular bone images by a TV box approach. , 2015, , .		0
35	Volumetric femoral BMD, bone geometry, and serum sclerostin levels differ between type 2 diabetic postmenopausal women with and without fragility fractures. Osteoporosis International, 2015, 26, 1283-1293.	3.1	54
36	Spatial distribution of intracortical porosity varies across age and sex. Bone, 2015, 75, 88-95.	2.9	38

Andrew J Burghardt

#	Article	IF	CITATIONS
37	Automatic multi-parametric quantification of the proximal femur with quantitative computed tomography. Quantitative Imaging in Medicine and Surgery, 2015, 5, 552-68.	2.0	23
38	Bone Structure and Perfusion Quantification of Bone Marrow Edema Pattern in the Wrist of Patients with Rheumatoid Arthritis: A Multimodality Study. Journal of Rheumatology, 2014, 41, 1766-1773.	2.0	14
39	Novel anthropomorphic hip phantom corrects systemic interscanner differences in proximal femoral vBMD. Physics in Medicine and Biology, 2014, 59, 7819-7834.	3.0	9
40	The influence of disuse on bone microstructure and mechanics assessed by HR-pQCT. Bone, 2014, 63, 132-140.	2.9	66
41	Improved Trabecular Bone Structure of 20-Month-Old Male Spontaneously Hypertensive Rats. Calcified Tissue International, 2014, 95, 282-291.	3.1	8
42	Quantification of lower leg arterial calcifications by high-resolution peripheral quantitative computed tomography. Bone, 2014, 58, 42-47.	2.9	25
43	Three-dimensional analysis of subchondral cysts in hip osteoarthritis: An ex vivo HR-pQCT study. Bone, 2014, 66, 140-145.	2.9	28
44	Postmenopausal women treated with combination parathyroid hormone (1–84) and ibandronate demonstrate different microstructural changes at the radius vs. tibia: the PTH and Ibandronate Combination Study (PICS). Osteoporosis International, 2013, 24, 2591-2601.	3.1	28
45	High-Resolution Peripheral Quantitative Computed Tomography for the Assessment of Bone Strength and Structure: A Review by the Canadian Bone Strength Working Group. Current Osteoporosis Reports, 2013, 11, 136-146.	3.6	182
46	Quantitative In Vivo HR-pQCT Imaging of 3D Wrist and Metacarpophalangeal Joint Space Width in Rheumatoid Arthritis. Annals of Biomedical Engineering, 2013, 41, 2553-2564.	2.5	60
47	Increased cortical porosity in type 2 diabetic postmenopausal women with fragility fractures. Journal of Bone and Mineral Research, 2013, 28, 313-324.	2.8	369
48	Computational identification and quantification of trabecular microarchitecture classes by 3-D texture analysis-based clustering. Bone, 2013, 54, 133-140.	2.9	23
49	Heterogeneity of bone microstructure in the femoral head in patients with osteoporosis: An ex vivo HR-pQCT study. Bone, 2013, 56, 139-146.	2.9	33
50	Age- and gender-related differences in cortical geometry and microstructure: Improved sensitivity by regional analysis. Bone, 2013, 52, 623-631.	2.9	51
51	Structural analysis of cortical porosity applied to HR-pQCT data. Medical Physics, 2013, 41, 013701.	3.0	29
52	Multicenter precision of cortical and trabecular bone quality measures assessed by high-resolution peripheral quantitative computed tomography. Journal of Bone and Mineral Research, 2013, 28, 524-536.	2.8	98
53	Quantitative and Semiquantitative Bone Erosion Assessment on High-resolution Peripheral Quantitative Computed Tomography in Rheumatoid Arthritis. Journal of Rheumatology, 2013, 40, 408-416.	2.0	41
54	The effect of voxel size on highâ€resolution peripheral computed tomography measurements of trabecular and cortical bone microstructure. Medical Physics, 2012, 39, 1893-1903.	3.0	96

#	Article	IF	CITATIONS
55	Visual grading of motion induced image degradation in high resolution peripheral computed tomography: Impact of image quality on measures of bone density and micro-architecture. Bone, 2012, 50, 111-118.	2.9	223
56	Imaging longitudinal changes in articular cartilage and bone following doxycycline treatment in a rabbit anterior cruciate ligament transection model of osteoarthritis. Magnetic Resonance Imaging, 2012, 30, 271-282.	1.8	17
57	Vascular patterning and permeability in prostate cancer models with differing osteogenic properties. NMR in Biomedicine, 2012, 25, 843-851.	2.8	3
58	Does vertebral bone marrow fat content correlate with abdominal adipose tissue, lumbar spine bone mineral density, and blood biomarkers in women with type 2 diabetes mellitus?. Journal of Magnetic Resonance Imaging, 2012, 35, 117-124.	3.4	196
59	Morphology of the human vertebral endplate. Journal of Orthopaedic Research, 2012, 30, 280-287.	2.3	121
60	Longitudinal evaluation of the effects of alendronate on MRI bone microarchitecture in postmenopausal osteopenic women. Bone, 2011, 48, 611-621.	2.9	47
61	Quantitative characterization of subject motion in HR-pQCT images of the distal radius and tibia. Bone, 2011, 48, 1291-1297.	2.9	88
62	Trabecular Reorganization in Consecutive Iliac Crest Biopsies when Switching from Bisphosphonate to Strontium Ranelate Treatment. PLoS ONE, 2011, 6, e23638.	2.5	12
63	Human Disc Nucleus Properties and Vertebral Endplate Permeability. Spine, 2011, 36, 512-520.	2.0	90
64	Noninvasive imaging of bone microarchitecture. Annals of the New York Academy of Sciences, 2011, 1240, 77-87.	3.8	56
65	High-resolution Computed Tomography for Clinical Imaging of Bone Microarchitecture. Clinical Orthopaedics and Related Research, 2011, 469, 2179-2193.	1.5	213
66	Ultrashort echo time MRI of cortical bone at 7 tesla field strength: A feasibility study. Journal of Magnetic Resonance Imaging, 2011, 34, 691-695.	3.4	29
67	Variations in morphological and biomechanical indices at the distal radius in subjects with identical BMD. Journal of Biomechanics, 2011, 44, 257-266.	2.1	44
68	High-Resolution Imaging Techniques for Bone Quality Assessment. , 2011, , 891-925.		1
69	Age- and gender-related differences in the geometric properties and biomechanical significance of intracortical porosity in the distal radius and tibia. Journal of Bone and Mineral Research, 2010, 25, 983-993.	2.8	271
70	Assessment of trabecular bone structure using MDCT: comparison of 64- and 320-slice CT using HR-pQCT as the reference standard. European Radiology, 2010, 20, 458-468.	4.5	52
71	A longitudinal HR-pQCT study of alendronate treatment in postmenopausal women with low bone density: Relations among density, cortical and trabecular microarchitecture, biomechanics, and bone turnover. Journal of Bone and Mineral Research, 2010, 25, 2558-2571.	2.8	210
72	High-Resolution Peripheral Quantitative Computed Tomographic Imaging of Cortical and Trabecular Bone Microarchitecture in Patients with Type 2 Diabetes Mellitus. Journal of Clinical Endocrinology and Metabolism, 2010, 95, 5045-5055.	3.6	407

Andrew J Burghardt

#	Article	IF	CITATIONS
73	High-Resolution Imaging Techniques for the Assessment of Osteoporosis. Radiologic Clinics of North America, 2010, 48, 601-621.	1.8	174
74	Higher doses of bisphosphonates further improve bone mass, architecture, and strength but not the tissue material properties in aged rats. Bone, 2010, 46, 1267-1274.	2.9	38
75	Contribution of the intra-specimen variations in tissue mineralization to PTH- and raloxifene-induced changes in stiffness of rat vertebrae. Bone, 2010, 46, 1162-1169.	2.9	29
76	Regional variations of gender-specific and age-related differences in trabecular bone structure of the distal radius and tibia. Bone, 2010, 46, 1652-1660.	2.9	66
77	Reproducibility of direct quantitative measures of cortical bone microarchitecture of the distal radius and tibia by HR-pQCT. Bone, 2010, 47, 519-528.	2.9	397
78	Trabecular Bone Structure Analysis in the Osteoporotic Spine Using a Clinical In Vivo Setup for 64-Slice MDCT Imaging: Comparison to μCT Imaging and μFE Modeling. Journal of Bone and Mineral Research, 2009, 24, 1628-1637.	2.8	38
79	Assessment of trabecular bone structure of the calcaneus using multi-detector CT: Correlation with microCT and biomechanical testing. Bone, 2009, 44, 976-983.	2.9	65
80	Accuracy of volumetric bone mineral density measurement in high-resolution peripheral quantitative computed tomography. Bone, 2009, 45, 473-479.	2.9	41
81	In Vivo Determination of Bone Structure in Postmenopausal Women: A Comparison of HR-pQCT and High-Field MR Imaging. Journal of Bone and Mineral Research, 2008, 23, 463-474.	2.8	122
82	Quantitative Assessment of Bone Tissue Mineralization with Polychromatic Micro-Computed Tomography. Calcified Tissue International, 2008, 83, 129-138.	3.1	89
83	In vivo ultraâ€highâ€field magnetic resonance imaging of trabecular bone microarchitecture at 7 T. Journal of Magnetic Resonance Imaging, 2008, 27, 854-859.	3.4	63
84	Resolution Dependence of the Non-metric Trabecular Structure Indices. Bone, 2008, 42, 728-736.	2.9	67
85	Evaluation of fetal bone structure and mineralization in IGF-I deficient mice using synchrotron radiation microtomography and Fourier transform infrared spectroscopy. Bone, 2007, 40, 160-168.	2.9	28
86	Wavelet-based characterization of vertebral trabecular bone structure from magnetic resonance images at 3 T compared with micro-computed tomographic measurements. Magnetic Resonance Imaging, 2007, 25, 392-398.	1.8	22
87	The Effects of Geometric and Threshold Definitions on Cortical Bone Metrics Assessed by In Vivo High-Resolution Peripheral Quantitative Computed Tomography. Calcified Tissue International, 2007, 81, 364-371.	3.1	50
88	A Local Adaptive Threshold Strategy for High Resolution Peripheral Quantitative Computed Tomography of Trabecular Bone. Annals of Biomedical Engineering, 2007, 35, 1678-1686.	2.5	104
89	Sensitivity of damage predictions to tissue level yield properties and apparent loading conditions. Journal of Biomechanics, 2001, 34, 699-706.	2.1	34